Fault ride-through performance evaluation of an interleaved grid-connected converter employing low switching frequency

Bede, Lorand; Gohil, Ghanshyamsinh Vijaysinh; Ciobotaru, M.; Kerekes, Tamas; Teodorescu, Remus; Agelidis, V. G.

Published in:
Proceedings of the 31st Annual IEEE Applied Power Electronics Conference and Exposition (APEC)

DOI (link to publication from Publisher):
10.1109/APEC.2016.7468096

Publication date:
2016

Document Version
Publisher's PDF, also known as Version of record

Fault Ride-Through Performance Evaluation of an Interleaved Grid-Connected Converter Employing Low Switching Frequency

Lorand Bede[1], Ghanshyamsihn Gohil[1], Mihai Ciobotaru[2], Tamas Kerekes[1], Remus Teodorescu[1], Vassilios G Agelidis[2]
[1]Department of Energy Technology,Aalborg University, Aalborg, Denmark
[2]School of Electrical Engineering, University of New South Wales, Sydney, Australia
Email: lbe@et.aau.dk

***Abstract*—This paper presents the performance evaluation under grid voltage sags of a two parallel-interleaved grid-connected converters employing low switching frequency. A current controller based on the synchronous reference frame including voltage feed-forward is used. The dominant frequency components from the direct- and quadrature-axis voltage V_d and V_q are eliminated by using an adaptive moving average filter. The dynamic performance of the converter during voltage sags is improved using an adaptive approach which minimizes the filter delay during the faults. The presented results conclude the performance of the converter system.**

Keywords—feed forward filtering, low switching, grid connected, grid control, LVRT, parallel interleaved,

I. INTRODUCTION

In the last decades the percentage of the renewable energy sources contributing to the energy production has increased significantly [1].To ensure stable grid operation more and more stringent grid codes are introduced, one of the most stringent one being the German BDEW standard [2]. Traditionally, in order to comply with the grid codes, a Voltage Source Converter (VSC) is employed [1]. In order to maintain low switching losses, the switching frequency (f_{sw}) of the VSCs has to be limited to a few kHz in the case of MW size power electronic converters. Furthermore, high order filters (i.e. *LCL*) are usually employed at the output of the converter[1], to be able to comply with the stringent standard requirements.

In general, the power converters of large-scale renewable energy power plants are often connected to the medium voltage network to reduce transmission losses. Since the operating voltage for these converters is limited, a step up transformer is required when connecting to medium voltage line. Furthermore, the leakage inductance of this transformer can be used as the grid side inductor of an *LCL* filter [3].

Multiple power converters can be connected in parallel to increase the power handling capability of these converter systems [4]. To reduce the filtering requirements, carrier interleaving can be employed [5]. By interleaving the carriers, the first order switching harmonic is removed from the total current [6]. On the other hand, carrier interleaving causes an additional circulating current to flow between the modules of the converters connected in parallel [7]. To suppress this circulating current, multiple solutions are available [8, 9]. In this paper a coupled inductor (CI) is added between the corresponding phases of the converters to limit the circulating current[10, 11].

There are different methods on how to control the converter current injected into the grid [12, 13]. The most common method is to use a Proportional Integral (PI) controller in the synchronous reference frame. It has been proven that, if the direct and quadrature axis voltage (V_d and V_q) is fed-forward to the output of the PI controller, the performance of the PI controller is enhanced during grid voltage transients [14]. A Phased-Locked Loop (PLL) is used to obtain the angle of the grid voltage which is measured at the Point of Common Coupling (PCC) [15, 16]. There are two connection points where the grid voltage can be measured depending on whether a step up transformer is used or not. One solution is to measure the voltage on the medium voltage side of the transformer. This solution is not preferred since the medium voltage sensors are expensive. The preferred solution is to measure the voltage on the low voltage side of the transformer. By doing so, the voltage will be measured across the capacitor of the output filter, in the case when *LCL* filters are used. However, the voltage across the capacitor is distorted and it contains multiple harmonics owing to the modulation technique. On the other hand, V_d and V_q should not contain any harmonics, otherwise the harmonic performance of the system might be compromised. A filter can be used to filter V_d and V_q accordingly. Nevertheless, the filter will introduce delays, which could affect the converter dynamics during voltage sags.

This paper evaluates the fault ride-through capability of a grid-connected converter employing low switching frequency. An adaptive Moving Average Filter (MAF) is used, which eliminates the dominant frequency components from V_d and V_q. This filter has the ability to minimize its delay during voltage sags, thus helping the dynamic performance of the converter system.

II. SYSTEM DESCRIPTION

A. Converter system

A system consisting of two 2-level parallel interleaved converters using full bridge topology and IGBTs was considered in this paper, as presented in Fig. 1.

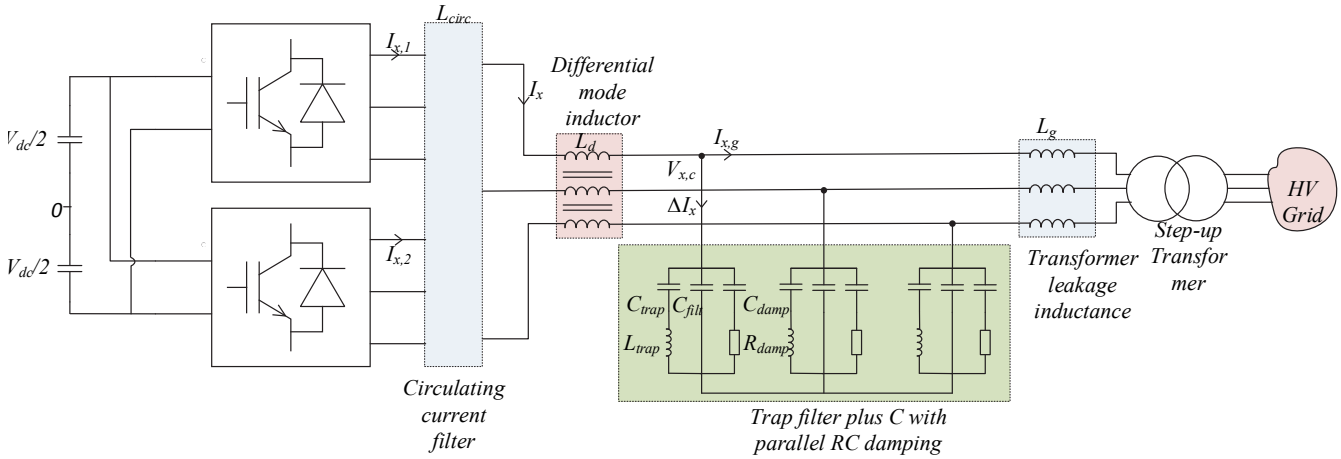

Fig. 1Schematic of the investigated converter system

Furthermore, three CIs were used (one for each phase) to limit the circulating currents caused by the interleaving.

Due to the interleaving, the major high frequency component in the total current (I_x, where x= [a,b,c]) is at the double of the switching frequency. A trap filter is designed to eliminate this frequency component from the grid current ($I_{x,g}$)[17]. Along with the trap filter, an *LCL* filter with passive damping is used. The leakage inductance of the step-up transformer, which is used to be able to connect to the medium voltage network, acts as the grid side inductor of the *LCL* filter.

B. Control system

The current control uses PI controllers in synchronous reference frame. A three-phase PLL provides the voltage phase angle used to obtain the direct and quadrature axis components of the grid currents(I_d, I_q) and PCC voltage (V_d, V_q), respectively. During the voltage sags, it is critical to have an accurate feed-forward value of V_d and V_q to help the converter dynamics. In the case when no feed-forward is used or an incorrect value is fed-forward, the current drawn from the converter will increase rapidly and the converter may trip. The rapid increase in current is due to the low controller bandwidth as a result of low switching frequency. On the other hand, some of the grid standards require the converter to stay connected during grid voltage sags and support the network. Therefore, the tripping of the converter in this situation should be avoided.

The structure of the control system is presented in Fig. 2. The three phase voltages are sampled at the capacitor of the filter, and they are fed to the PLL block. The PLL block calculates the grid angle (θ) and the direct and quadrature components of the voltage (V_d and V_q).

These values are used as inputs to the filter, which can be either a Moving Average Filter (MAF) or an Adaptive MAF (AMAF). The filtered values (V_{d_filt} and V_{q_filt}) are fed forward to the output of the current controller for the corresponding phase.

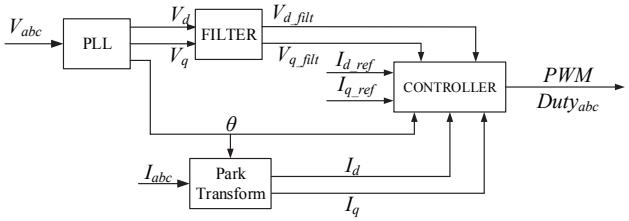

Fig. 2Software structure of the three-phase converter system.

C. Moving Average Filter

An MAFis designed to filter the major harmonic components from V_d and V_q, which are fed-forward to the controller. Thus, there is a need for two filters, one to filter the V_d and one to filter the V_q.

The filter cut-off frequency is tuned to remove the 300 Hz and its upper order harmonics caused by the modulation. The equation of this filter [16] is represented by

$$h[n] = \frac{1}{N}\sum_{k=0}^{N-1}\delta[n-k] \tag{1}$$

where h is the output vector of the filter, δ is the input vector of the filter, and N is the number of samples used for averaging. The value of N can be determined as follows:

$$N = floor(\frac{1}{f_{cut}\cdot T_s}) \tag{2}$$

where f_{cut} is the frequency to be filtered, and T_s is the sampling period. Since the double update technique is used here, the value of T_s is $1/(2*f_{sw})$.

The equation of the MAF is as follows:

$$\frac{1}{N}\sum_{k=0}^{N-1}V_{x\_sampled}[n-k] \tag{3}$$

where x represents the *d* and the *q* axis.

The drawback of this solution is that during transient operations, such as voltage sags, the filter introduces a delay which will affect the transient response of the system.

D. Adaptive Moving Average Filter

In order to overcome the shortcomings of the MAF, this paper proposes an Adaptive MAF (AMAF) which enhances the transient performance of the system, and in the same time has the same performance in steady state as the MAF.

A simple algorithm is used to detect voltage sags based on previous samples and to adapt the feed-forward value to the new conditions, as shown by(4). The algorithm compares the actual measured value with the previously measured one and if the difference between the two samples is bigger than a predefined value the algorithm interprets it as a fault.

$$V_{x\_filt} = \begin{cases} \frac{1}{N}\sum_{k=0}^{N-1} V_{x\_sampled}[n-k] & if\ no\ fault \\ V_{x\_sampled} & if\ fault \end{cases} \quad (4)$$

To ensure a fast tracking of the V_d and V_q, the algorithm sets the feed-forward value to the actual V_d and V_q (without any filtering) during the voltage sag.

III. RESULTS

A. Experimental results

To test the performance of the MAF and the AMAF an experimental setup consisting of 2 parallel interleaved converters has been built. The total power of the system is 10KW and the control system has been implemented on a Texas Instruments TMS320F28346 floating point Micro Controller Unit (MCU). The parameters of the filter components along with other system parameters are presented in TABLE I. The switching frequency used is 2.55 kHz. Due to the limited switching frequency, the bandwidth of the controller is also limited. In this system the interleaving technique is used, hence the output of each converter is connected to 3 CIs, in order to limit the circulating current between the converters. In this case the voltage to which the synchronization is made is measured at the filter capacitance. This is done because in the high power setup the MV voltages would be too expensive to measure. The drawback of this measurement is that the measured voltage will be distorted and will contain a lot of harmonics. Since the paper wants to comply with the BDEW standard, a trap filter is employed, which is tuned to eliminate the second carrier harmonics from the grid current.

The following three cases have been investigated in order to determine the performance of the system under a symmetrical grid fault, when the grid voltage is dropped to 25% of its nominal value: 1) when no filtering was applied on the V_d and V_q values, 2) When the MAF was used and 3) When the AMAF was used. The comparison criteria has been the current Total Harmonic Distortion (THD) in steady state and the current overshoot during the transient operation. Furthermore, to show the effectiveness of the filter at the specific harmonic components the FFT analysis is also included up to 1Khz.

For all three cases the measured currents and voltages are shown. For a better understanding, the direct and quadrature axis component of both the currents and voltages are also presented. To be able to make a fair comparison, for all three cases the grid faults happened at the same instance (at the same grid angle). This was possible by using a grid emulator from California Instruments.

TABLE I System Parameters

Parameter	Value
Power	10KW
Nominal Frequency	50 Hz
Switching Frequency	2.55 KHz
Nominal Voltage	230 Vrms
DC link Voltage(V_{DC})	650V
Differential mode inductor(L_d)	2.2 mH
Trap capacitance (C_{trap})	4.4 µF
Trap inductance (L_{trap})	232 µH
Damping Capacitance (C_{damp})	2.2 µF
Damping Resistance(R_{damp})	30 Ω
Filter Capacitance (C_f)	2.2 µF
Grid side inductance (L_g)	3.6 mH

1) No filtering of the feed forward terms

In this case the measured V_d and V_q components of the grid voltage have been fed forward to the output of the I_d and I_q current controllers.

The experimental results showing the grid currents and the grid voltages are shown by Fig. 3 and Fig. 4, respectively. As it is visible from the grid currents (Fig. 3), during steady state in the currents there are dominant harmonics such as the 5th and the 7th. Because of this the THD value of the currents is ~ 5%. Moreover, during the voltage sag the currents start to oscillate and this oscillation is damped only after a fundamental period. The capacitor voltages corresponding to the grid currents shown previously are depicted by Fig. 4. It has to be noted that the capacitor voltages contain double switching harmonics because of the high order filter.

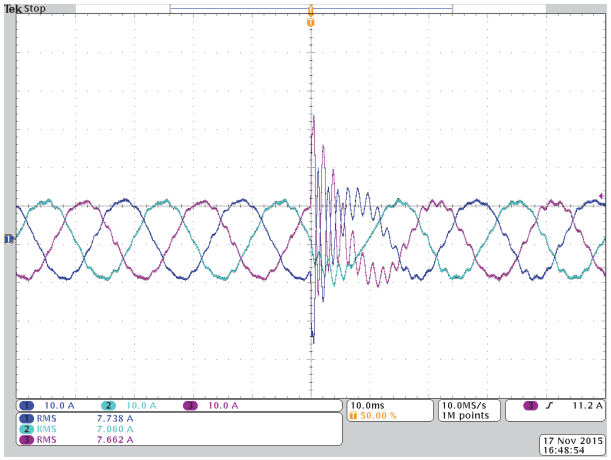

Fig. 3 Grid currents when no filtering is applied for V_d; Ch1(*blue*) grid current Phase A ($I_{A,g}$),Ch2(*cyan*) grid current Phase B ($I_{B,g}$),Ch3(*magenta*) grid current Phase C ($I_{C,g}$)

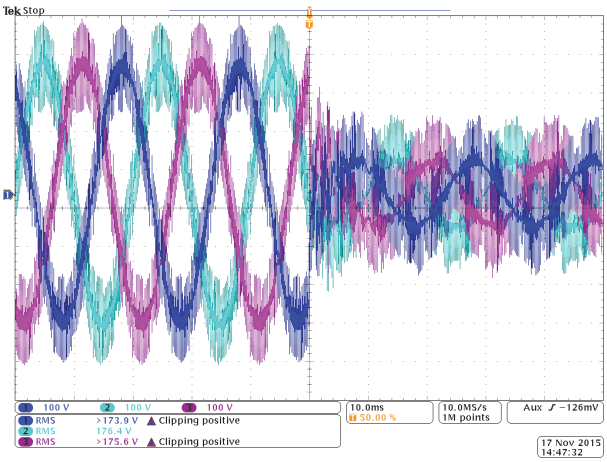

Fig. 4 Voltage on the filter capacitor with no feed filtering on the V_d;Ch1 (*blue*) Capacitor voltage Phase A ($V_{A,c}$),Ch2(*cyan*) Capacitor voltage Phase B ($V_{B,c}$),Ch3(*magenta*) Capacitor voltage Phase C ($V_{C,c}$)

2) *MAF of the feed forward terms*

In this case the value of V_d and V_q are fed to the controller after they have been filtered by the MAF. The system in steady state and during transient operation is depicted by the current and voltage waveform on Fig. 5 and Fig. 6, respectively.

In this case the THD value of current during steady state operation has been decreased from ~5% to ~3%. Moreover, unlike in the previous case, during the voltage sag the current is free from high frequency resonances. On the other hand, because of the filtering the overshoot is higher by 25%.

3) *AMAF of the feed forward terms*

The purpose of this filtering is to have the steady state behavior of the MAF and in the same time have fast transient response. During steady state the AMAF acts as a MAF, and because of this the current THD is only ~3%. However, when the algorithm detects that a fault happened, the filtering is suspended and the feed forward values are the measured ones

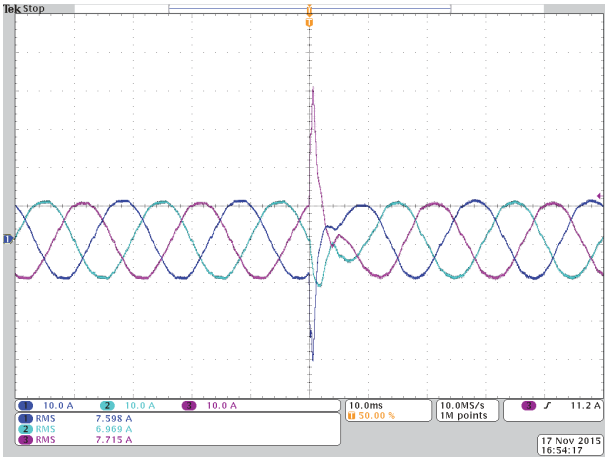

Fig. 5 Grid currents when the MAF is applied for V_d;Ch1(*blue*) grid current Phase A ($I_{A,g}$),Ch2(*cyan*) grid current Phase B ($I_{B,g}$),Ch3(*magenta*) grid current Phase C ($I_{C,g}$)

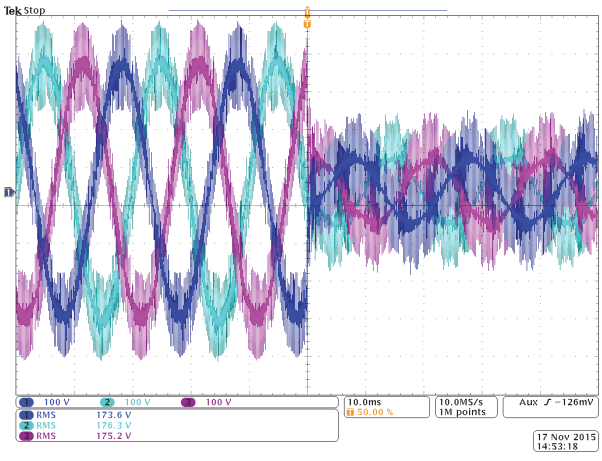

Fig. 6 Voltage on the filter capacitor when the Vd was filtered with the MAF;Ch1 (*blue*) Capacitor voltage Phase A ($V_{A,c}$),Ch2(*cyan*) Capacitor voltage Phase B ($V_{B,c}$),Ch3(*magenta*) Capacitor voltage Phase C ($V_{C,c}$)

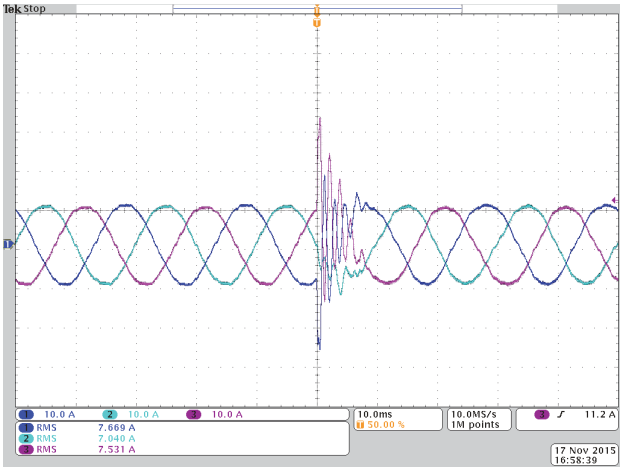

Fig. 7 Grid currents when the AMAF is applied for V_d;Ch1(*blue*) grid current Phase A ($I_{A,g}$),Ch2(*cyan*) grid current Phase B ($I_{B,g}$),Ch3(*magenta*) grid current Phase C ($I_{C,g}$)

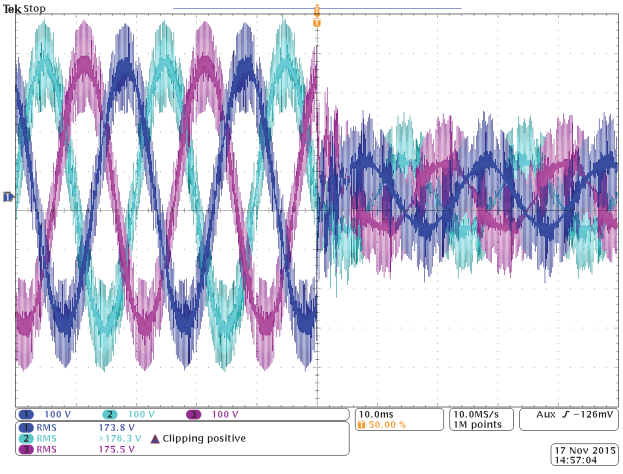

Fig. 8 Voltage on the filter capacitor when the Vd was filtered with the AMAF;Ch1 (*blue*) Capacitor voltage Phase A ($V_{A,c}$),Ch2(*cyan*) Capacitor voltage Phase B ($V_{B,c}$),Ch3(*magenta*) Capacitor voltage Phase C ($V_{C,c}$)

without any filtering. This can be seen from the current and voltage values in Fig. 7 and Fig. 8, respectively. During transient the same performance is observable as in the case where no filtering has been used, while in steady state the current THD is the same as in the case of the MAF.

IV. Discussion

For a better understanding, the direct and quadrature axis voltages (V_d and V_q) and currents (I_d and I_q) were obtained and are depicted by Fig. 10 and Fig. 11, respectively.

A. Steady state operation

In order to quantify the effectiveness of the MAF, the THD levels of the currents have been compared. In the case when there was no filtering applied (Fig. 3) the THD value of the current was ~5%, while in the case when the MAF was applied (Fig. 5) the current THD decreased to ~3%. The same THD value (~3%) was also obtained for the AMAF case. Furthermore, on Fig. 9 the Fast Fourier Transform (FFT) of the grid currents during steady state operation are shown, for all 3 above mentioned cases. For the MAF and AMAF cases the dominant harmonic components are reduced significantly compared to the non-filtered case. As mentioned before, the AMAF filter works as the MAF during steady-state operations as it is also visible from Fig. 9.

B. Transient operation

During the fault, when there is no filtering applied on the V_d and V_q, the grid current starts to oscillate. This phenomenon is also visible from the direct and quadrature axis current plots (Fig. 10, blue lines). However, in the case of the MAF, the current oscillation is removed, but the overshoot of the currents is higher (Fig. 7). From Fig. 10 (red lines) it is visible that the overshoot of the I_d is higher than in the non-filtered case. Moreover, the transient response is also slower. As for the I_q, the oscillation is also removed from this current, but the overshoot is much smaller compared to the non-filtered one.

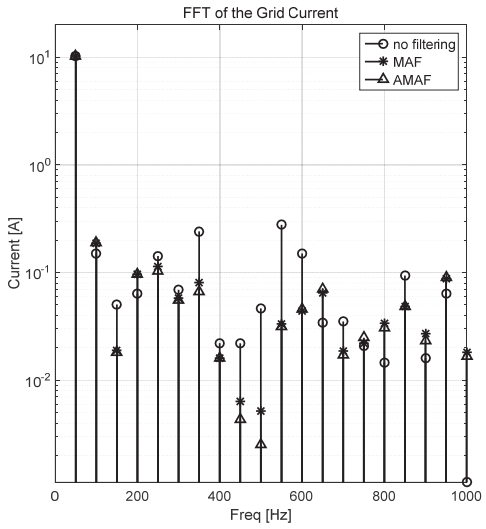

Fig. 9 FFT of the grid current for the 3 investigated cases (with no filtering, MAF and AMAF)

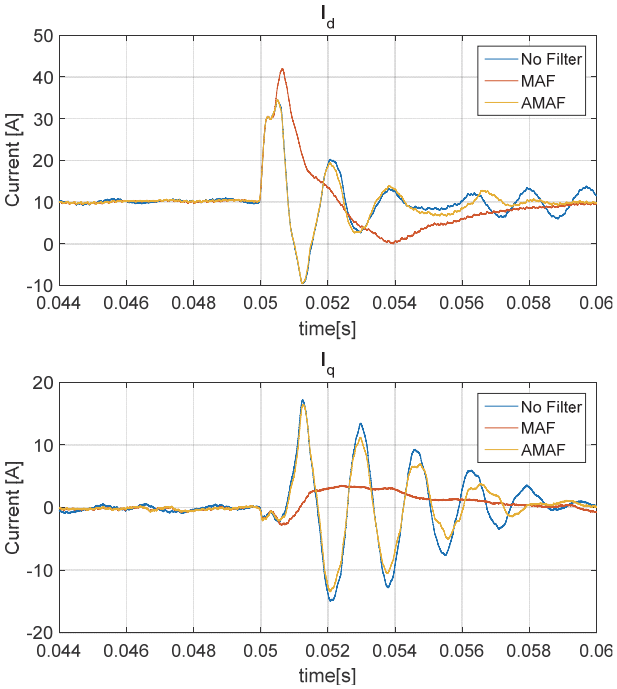

Fig. 10 I_d(top) and I_q(bottom) currents for the 3 different cases; *Blue*—no filter; *Red*—MAF; *Orange*—AMAF

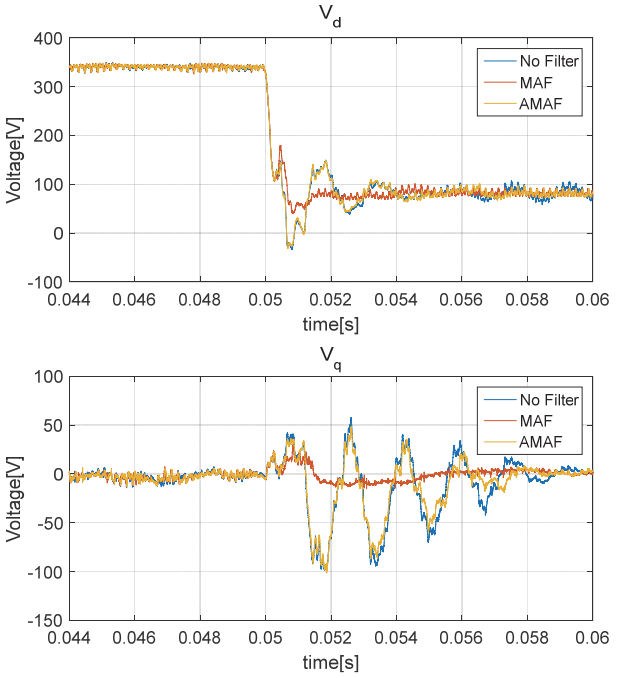

Fig. 11 V_d(top) and V_q(bottom) parts of the capacitor voltages; *Blue*—no filter; *Red*—MAF; *Orange*—AMAF

V. CONCLUSIONS

This paper uses a MAF in order to eliminate the harmonics from the grid current, which are caused by modulation and by the feed-forward of the grid voltages, which can contain also harmonics. This is done by filtering the V_d and V_q values which are used for the feed-forward part of the current controllers. The shortcoming of this method is that during transients the response of the control system will be increased along with the current overshoot. The overshoot of the grid current has been increased by 25%. To overcome this limitation the paper proposes an AMAF, which has the same performance as the MAF during steady state operation, but during transient the filtering is suspended and a faster response can be achieved (compared to the MAF). Moreover, the overshoot is also decreased, hence the proposed method helps the control system during transients to be able to remain connected.

An FFT analysis of the grid current has also been presented for the 3 cases, where the individual harmonics are presented up until 1 kHz. It is visible from the graph that the dominant frequency components in the grid current are decreased significantly in the case when either of the filtering has been applied.

A setup consisting of two parallel interleaved converters has been built, and the methods were tested on this system. The experimental results reflect the performance of the filtering method both in steady state and during transient operations.

REFERENCES

[1] F. Blaabjerg, M. Liserre, and M. Ke, "Power Electronics Converters for Wind Turbine Systems," *Industry Applications, IEEE Transactions on,* vol. 48, pp. 708-719, 2012.

[2] B. B. d. Energieund and Wasserwirtschaft e.V., "Technical guidline: Generating plants connected to the medium-voltage network," ed, 2008.

[3] G. Gohil, L. Bede, R. Teodorescu, T. Kerekes, and F. Blaabjerg, "Line Filter Design of Parallel Interleaved VSCs for High Power Wind Energy Conversion System," *Power Electronics, IEEE Transactions on,* vol. PP, pp. 1-1, 2015.

[4] B. Andresen and J. Birk, "A high power density converter system for the Gamesa G10x 4,5 MW wind turbine," in *Power Electronics and Applications, 2007 European Conference on*, 2007, pp. 1-8.

[5] J. S. S. Prasad and G. Narayanan, "Minimization of Grid Current Distortion in Parallel-Connected Converters Through Carrier Interleaving," *Industrial Electronics, IEEE Transactions on,* vol. 61, pp. 76-91, 2014.

[6] S. K. T. Miller, T. Beechner, and S. Jian, "A Comprehensive Study of Harmonic Cancellation Effects in Interleaved Three-Phase VSCs," in *Power Electronics Specialists Conference, 2007. PESC 2007. IEEE*, 2007, pp. 29-35.

[7] R. Maheshwari, G. Gohil, L. Bede, and S. Munk-Nielsen, "Analysis and modelling of circulating current in two parallel-connected inverters," *Power Electronics, IET,* vol. 8, pp. 1273-1283, 2015.

[8] G. Gohil, L. Bede, R. Teodorescu, T. Kerekes, and F. Blaabjerg, "An Integrated Inductor For Parallel Interleaved Three-Phase Voltage Source Converters," *Power Electronics, IEEE Transactions on,* vol. PP, pp. 1-1, 2015.

[9] G. Gohil, L. Bede, R. Teodorescu, T. Kerekes, and F. Blaabjerg, "An Integrated Inductor for Parallel Interleaved VSCs and PWM Schemes for Flux Minimization," *Industrial Electronics, IEEE Transactions on,* vol. PP, pp. 1-1, 2015.

[10] G. J. Capella, J. Pou, S. Ceballos, J. Zaragoza, and V. G. Agelidis, "Current-Balancing Technique for Interleaved Voltage Source Inverters With Magnetically Coupled Legs Connected in Parallel," *Industrial Electronics, IEEE Transactions on,* vol. 62, pp. 1335-1344, 2015.

[11] F. Forest, E. Laboure, T. A. Meynard, and V. Smet, "Design and Comparison of Inductors and Intercell Transformers for Filtering of PWM Inverter Output," *Power Electronics, IEEE Transactions on,* vol. 24, pp. 812-821, 2009.

[12] A. Timbus, M. Liserre, R. Teodorescu, P. Rodriguez, and F. Blaabjerg, "Evaluation of Current Controllers for Distributed Power Generation Systems," *Power Electronics, IEEE Transactions on,* vol. 24, pp. 654-664, 2009.

[13] L. Bede, G. Gohil, T. Kerekes, M. Ciobotaru, R. Teodorescu, and V. G. Agelidis, "Comparison between grid side and inverter side current control for parallel interleaved grid connected converters," in *Power Electronics and Applications (EPE'15 ECCE-Europe), 2015 17th European Conference on*, 2015, pp. 1-10.

[14] F. Blaabjerg, R. Teodorescu, M. Liserre, and A. V. Timbus, "Overview of Control and Grid Synchronization for Distributed Power Generation Systems," *Industrial Electronics, IEEE Transactions on,* vol. 53, pp. 1398-1409, 2006.

[15] P. Rodriguez, A. Luna, M. Ciobotaru, R. Teodorescu, and F. Blaabjerg, "Advanced Grid Synchronization System for Power Converters under Unbalanced and Distorted Operating Conditions," in *IEEE Industrial Electronics, IECON 2006 - 32nd Annual Conference on*, 2006, pp. 5173-5178.

[16] S. Golestan, M. Ramezani, J. M. Guerrero, F. D. Freijedo, and M. Monfared, "Moving Average Filter Based Phase-Locked Loops: Performance Analysis and Design Guidelines," *Power Electronics, IEEE Transactions on,* vol. 29, pp. 2750-2763, 2014.

[17] G. Gohil, L. Bede, R. Teodorescu, T. Kerekes, and F. Blaabjerg, "Design of the trap filter for the high power converters with parallel interleaved VSCs," in *Industrial Electronics Society, IECON 2014 - 40th Annual Conference of the IEEE*, 2014, pp. 2030-2036.